THE JOURNAL OF BIOLOGICAL CHEMISTRY
Vol. 279, No. 35, Issue of August 27, pp. 36546–36552, 2004
Printed in U.S.A.

Ca^{2+} Dependence of the Ca^{2+}-selective TRPV6 Channel*

Received for publication, April 27, 2004, and in revised form, June 4, 2004
Published, JBC Papers in Press, June 7, 2004, DOI 10.1074/jbc.M404679200

Matthias Bödding‡ and Veit Flockerzi

From the Experimentelle und klinische Pharmakologie und Toxikologie, Universität des Saarlandes, D-66421 Homburg, Germany

Microfluorimetry and patch-clamp experiments were performed on TRPV6-expressing HEK cells to determine whether this Ca^{2+}-sensing Ca^{2+} channel is constitutively active. Intact cells loaded with fura-2 had an elevated intracellular free Ca^{2+} concentration ($[Ca^{2+}]_i$), which decreased to the same level such as in non-transfected cells if external Ca^{2+} was chelated by EGTA. Whole cell recordings from non-transfected HEK cells and cells expressing human TRPV6 revealed the presence of a basal inward current in both types of cells when the internal solution contained 0.1 mM EGTA and 100 nM $[Ca^{2+}]_i$ or if the cytosolic Ca^{2+} buffering remained undisturbed in perforated patch-clamp experiments. If recombinantly expressed TRPV6 forms open channels, one would expect Ca^{2+}-induced current inhibition, because TRPV6 is negatively regulated by internal Ca^{2+}. However, dialyzing solutions with high $[Ca^{2+}]$ such as 1 μM into TRPV6-expressing cells did not block the basal inward current, which was not different from the recordings from non-transfected cells. In contrast, dialyzing 0.5 mM EGTA into TRPV6-expressing cells readily activated Ca^{2+} inward currents, which were undetectable in non-transfected cells. Interestingly, monovalent cations permeated the TRPV6 channels under conditions where no Ca^{2+} permeation was detectable, indicating that divalent cations block TRPV6 channels from the extracellular side. Like human TRPV6, the truncated human $TRPV6_{\Delta 695-725}$, which lacks the C-terminal domain required for Ca^{2+}-calmodulin binding, does not form constitutive active channels, whereas the human $TRPV6_{D542A}$, carrying a point mutation in the presumed pore region, does not function as a channel. In summary, no constitutive open TRPV6 channels were detected in patch-clamp experiments from transfected HEK cells. However, channel activity is highly regulated by intracellular and extracellular divalent cations.

Calcium is the most abundant cation in the human body. Most of it is bound in bones and teeth and only very little is ionized. Changes in the intracellular free Ca^{2+} concentration ($[Ca^{2+}]_i$)[1] regulate many physiological and pathological processes such as muscle contraction, secretion of neurotransmitters, cell cycle, and apoptosis. Given the importance of this messenger, it is necessary to understand how Ca^{2+} is absorbed from our diet. There are at least two ways how this can take place: either through tight junctions in a paracellular manner or across the apical and basolateral membranes via a transcellular pathway (1). Recently, two genes have been cloned from Ca^{2+}-transporting epithelia: TRPV5 from rabbit kidney (formerly called epithelial calcium channel (ECaC) (2)) and TRPV6 from rat intestine (formerly called calcium transporter CaT (3)). Both channels form constitutively open channels, are highly Ca^{2+} selective (4, 5), show Ca^{2+}-dependent feedback inhibition, and are expressed in a 1,25-dihydroxyvitamin D_3-dependent fashion (1, 6). These characteristics and particularly the finding that Ca^{2+} entry depends on the capacity of intracellular Ca^{2+} buffers fit well with the expected features of the so far unidentified channels responsible for Ca^{2+} absorption.

In the present study we wanted to determine whether the human TRPV6 proteins form constitutive open channels under physiological conditions. For this purpose patch-clamp experiments and measurements of the $[Ca^{2+}]_i$ with fura-2 were performed on HEK cells expressing TRPV6 or mutant channels. The data indicate that TRPV6 is not spontaneously active but opens at low $[Ca^{2+}]_i$ and closes at higher $[Ca^{2+}]_i$. This sensitivity is due to local effects of Ca^{2+} at the intracellular region of the pore. Moreover, under conditions where Ca^{2+} currents are non-detectable, the channel is available for the permeation by monovalent cations, indicating that TRPV6 channels are also blocked in the presence of extracellular divalent cations.

EXPERIMENTAL PROCEDURES

Cell Culture, Transfected cDNA, and Transfection—HEK-293 (1573-CRL) and RBL-1 cells (ATTC, 1378-CRL) were obtained from the American Type Culture Collection (ATCC, Manassas, VA) and cultured as previously described (7). Cells were transiently transfected with 4 μg of DNA in 5 ml of the PolyFect® reagents (Qiagen, Hilden, Germany). The bicistronic expression plasmid pdiCaT-L was constructed as described before (5) and contained the entire protein-coding regions of the b-variant of human TRPV6 (formerly CaT-Lb, DDBJ/EMBL/GenBank™, accession number CAC20417) followed by an internal ribosomal entry site (IRES) and the green fluorescent protein (GFP) cDNA. Cells were used 46 h after transient transfection for Western blot analysis and biotinylation experiments.

Site-directed Mutagenesis—Mutagenesis of the aspartate residue at positions 542 was carried out using the QuikChange™ site-directed mutagenesis kit (Stratagene, La Jolla, CA) as described. The point mutation was generated by using the following primer pairs for PCR: sense primer, 5′-CCT TAC CAT CAT CGC TGG CCC AGC C-3′; and antisense primer, 5′-G GCT GGG CCA GCG ATG ATG GTA AGG-3′. The PCR products of the mutated TRPV6 cDNA was subcloned from the pcDNA3 (Invitrogen, Karlsruhe, Germany) into the pCAGGS-IRES-GFP vector. The nucleotide sequences of the $TRPV6_{D542A}$ point mutant was verified by sequencing the complete insert on both strands, including the Kozak sequence and the transition sites into the vector. The truncated TRPV6 variant ($TRPV6_{\Delta 695-725}$) has been described previously (8).

Western Blot Analysis—Lysates were prepared from HEK-293 wild-

* The costs of publication of this article were defrayed in part by the payment of page charges. This article must therefore be hereby marked "*advertisement*" in accordance with 18 U.S.C. Section 1734 solely to indicate this fact.

‡ To whom correspondence should be addressed: Tel.: 49-6841-162-6242; Fax: 49-6841-162-6402; E-mail: matthias.boedding@uniklinik-saarland.de.

[1] The abbreviations used are: $[Ca^{2+}]_i$, intracellular free Ca^{2+} concentration; CaT, Ca^{2+} transporter; IRES, internal ribosomal entry site; GFP, green fluorescent protein; BAPTA, 1,2-bis(2-aminophenoxy)ethane-*N*,*N*,*N*′,*N*′-tetraacetic acid; PBS, phosphate-buffered saline; HEDTA, *N*-(2-hydroxyethyl)-ethylenediamine-*N*,*N*′,*N*′-triacetic acid; HEK, human embryonic kidney; I-V, current-voltage; RBL, rat basophilic leukemia; TRP, transient receptor potential; TRPV, TRP-subfamily V (vanilloid-receptor type); wt, wild type.

type cells and TRPV6- and $TRPV6_{D542A}$-expressing HEK cells. Cells were grown on small coverslips (3.5 cm in diameter) up to 80–90% confluency. After removing the medium and washing in the presence of 1× PBS lysis was initiated by the addition of 150 μl of gel loading buffer. Lysates (20 μl) were applied to a 8% SDS-polyacrylamide gel, and proteins were separated by electrophoresis and transferred to a nitrocellulose membrane (0.45 μm) by tank blotting (Bio-Rad, München, Germany) in the presence of 20% methanol at 350 mA for 1.5 h. The blot was stained with Ponceau red and incubated in 5% nonfat dry milk in TBS buffer in diameter, at 21 °C for 1 h followed by incubation in the presence of the affinity-purified rabbit polyclonal anti-TRPV6 antibody 429 (5 μg/ml (9)) at 4 °C overnight. After washing the blot three times with TBS buffer, it was incubated at room temperature for 1 h in the presence of a horseradish peroxidase-labeled secondary antibody (anti-mouse IgG at 1:30,000, Dianova, Hamburg, Germany) and the Renaissance Western blot chemiluminescence reagent (PerkinElmer Life Sciences).

Cell Surface Biotinylation—Non-transfected HEK-293 cells and cells transiently expressing TRPV6 (15 culture dishes, 3.5 cm in diameter, with cells at 80–90% confluency each) were placed on ice and washed twice with ice-cold PBS at pH 8 containing 1 mM $MgCl_2$ and 0.5 mM $CaCl_2$. Cells were then incubated for 30 min at 4 °C with sulfosuccinimidyl-6-(biotinamido)hexanoate (final concentration 0.5 mg/ml; Sulfo-NHS-LC-biotin from Perbio Science Deutschland GmbH, Bonn, Germany), freshly diluted in PBS containing Mg^{2+}/Ca^{2+}. Biotinylation was terminated by rinsing the dishes twice with PBS containing Mg^{2+}/Ca^{2+} and 0.1% bovine serum albumin, which quenches the unbound sulfosuccinimidyl-6-(biotinamido)hexanoate, and once with PBS pH 7.4 without Mg^{2+}/Ca^{2+}. Cells were collected from plates using PBS containing 2 mM EGTA. The harvested cells were centrifuged at 1000 × *g* and 4 °C for 5 min and resuspended in ice-cold lysis buffer (PBS, pH 7.4, containing 1% Triton X-100, 1 mM EDTA, and a mixture of protease inhibitors). The lysates were rotated at 4 °C for 30 min to further solubilize the proteins. Cellular debris was removed by centrifugation for 5 min at 1000 × *g* and 4 °C. Following measurement of the protein content of the cell extract, samples containing 600 μg of proteins were added to 150 μl of avidin-agarose beads, pre-equilibrated in the lysis buffer, and rotated for 3 h at 4 °C. The biotin-avidin agarose complexes were then harvested by centrifugation (1000 × *g* at 4 °C for 5 min) and washed four times with the lysis buffer supplemented with 0.25 M NaCl to give a final concentration 0.4 M NaCl. The beads were then resuspended in 60 μl of 2× Laemmli buffer and incubated at 37 °C for 30 min prior to SDS-PAGE.

Electrophysiological Recordings and Solutions—Patch-clamp experiments were performed in the whole cell configuration (10) using an EPC-9 amplifier (HEKA Elektronik, Lambrecht, Germany). Cells were measured 24–32 h after transfection in a modified Ringer's solution containing (in mM): 145 NaCl, 10 $CaCl_2$, 10 CsCl, 2.8 KCl, 2 $MgCl_2$, 10 HEPES, adjusted to pH 7.2 with NaOH. The divalent-free solution contained (in mM): 145 NaCl, 10 CsCl, 2.8 KCl, 10 EGTA, 10 HEPES, adjusted to pH 7.2 with NaOH. The external solution for the optical recordings contained either 2 mM $CaCl_2$ or 1 mM EGTA instead of 10 mM $CaCl_2$. Patch pipettes were pulled from borosilicate glass (Kimax®), were dipped with their tips in Sigmacote® to be coated, and had resistances between 2 and 3 MΩ when filled with the standard internal solution containing (in mM): 145 cesium glutamate, 10 HEPES, 8 NaCl, 1 $MgCl_2$, 2 Mg-ATP adjusted to pH 7.2 with CsOH. The $[Ca^{2+}]$ of the cesium glutamate-based solution was clamped to 100 nM by the addition of 10 mM EGTA and 3.64 mM $CaCl_2$ or 10 mM EDTA and 6.34 mM $CaCl_2$. HEDTA (10 mM) and $CaCl_2$ (2 mM) were used in the pipette solution to clamp the $[Ca^{2+}]$ at 1 μM. Perforated-patch recordings were performed with the standard intracellular solution supplemented with 100 μg ml^{-1} nystatin (11). The tips of the patch-pipettes were filled with nystatin-free internal solution. When challenged with step depolarizations, perforation of the membrane patch was indicated by characteristic changes of the capacitance transient and by a continuous decline of the input resistance. To standardize experiments, recordings were started when the input resistance fell to a value of 20 MΩ or less; this point was reached usually 5–10 min after gigaseal formation. The series resistances in tight seal, whole cell experiments were typically in the range of 5–10 MΩ. Currents were filtered using an 8-pole Bessel filter at 8 kHz and digitized at 100 μs. Voltage-clamp recordings were performed using ramps from −110 mV to 90 mV over 50 ms, which were applied every 2 s using PULSE software (HEKA Electronik) on a personal computer. The holding potential was −10 mV between ramps. Several parameters (capacitance, series resistance, and holding current) were displayed simultaneously at a slower rate (2 Hz) using the X-Chart display (HEKA Electronik). The membrane potential values were corrected for a 10-mV liquid junction potential. No additional voltage correction was performed for the experiments under divalent-free conditions. Osmolarities of external and internal solutions were checked using the Osmomat 030 (Gonotec, Berlin, Germany). No measurable differences were detected for the experiments with 1 μM free intracellular Ca^{2+}. All experiments were carried out at room temperature (20–23 °C). Internal solutions were kept on ice to minimize hydrolysis of ATP.

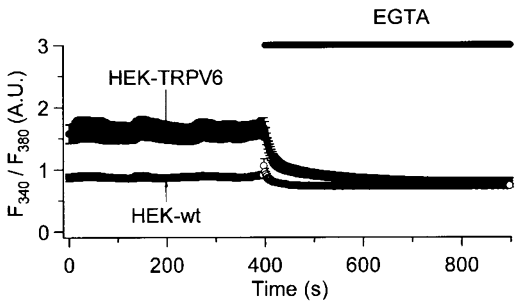

FIG. 1. **Fluorescent changes of the Ca^{2+} indicator dye fura-2 in TRPV6 expressing and non-transfected HEK cells when external Ca^{2+} is chelated by EGTA.** HEK cells were loaded with the fluorescent indicator fura-2 as described under "Experimental Procedures." The bath solution containing 2 mM Ca^{2+} was replaced by a 1 mM EGTA containing solution after 400 s as indicated by the *bar*. Mean data with double-sided S.E. are plotted *versus* time (n = 26 for HEK-TRPV6 and n = 17 for HEK-wt).

Microfluorimetry—Cells were incubated with the fluorescent Ca^{2+} indicator dye fura-2 AM (2 μM) at 37 °C for 30 min in the dark, and fluorescence intensity ratios (340/380 nm) were measured at 510 nm with the IMAGO system from T.I.L.L. Photonics (Martinsried, Germany) as previously described (12).

Data Analysis—Analysis was performed with PulseFit and programs written in the IGOR macro language (Wave Metrics, Lake Oswego, OR). Inward currents were measured at −80 mV without background current subtraction. Throughout, average data are given as means ± S.E. for a number (n) of cells. Student's t test was used for comparison of means.

Drugs—All chemicals were purchased from Sigma except fura-2 AM (Molecular Probes, Eugene, OR). Nystatin was dissolved in Me_2SO to yield a final concentration of 50 mg ml^{-1}, and these stock solutions were used for 1 day.

RESULTS

Elevated $[Ca^{2+}]_i$ in Fura-2 Ester-loaded TRPV6-expressing HEK Cells—Do the TRPV6 proteins form constitutive active Ca^{2+}-selective channels when expressed in HEK or RBL cells? This question was addressed by performing experiments with the Ca^{2+} indicator dye fura-2 on intact cells. The monitoring of the cytosolic Ca^{2+} concentration ($[Ca^{2+}]_i$) revealed an elevated $[Ca^{2+}]_i$ in HEK cells expressing TRPV6 in comparison to HEK cells that do not express TRPV6 (Fig. 1; F_{340}/F_{380} = 1.57 ± 0.15 arbitrary units, n = 26 for HEK-TRPV6 and F_{340}/F_{380} = 0.87 ± 0.06 arbitrary unit, n = 17 for HEK-wt). Replacement of extracellular Ca^{2+} (2 mM) by EGTA (1 mM) resulted in a pronounced decrease of the $[Ca^{2+}]_i$ in the TRPV6-expressing cells, whereas $[Ca^{2+}]_i$ of control cells decreased only slightly. With time, similar basal intracellular Ca^{2+} levels were reached in both cell types (Fig. 1; at 500 s after application: F_{340}/F_{380} = 0.80 ± 0.05 arbitrary unit, n = 26 for HEK-TRPV6 and F_{340}/F_{380} = 0.72 ± 0.03 arbitrary unit, n = 17 for HEK). Similar data have been reported previously, and it was concluded that TRPV6 forms constitutive open Ca^{2+} selective channels (5). Another explanation could be that TRPV6-mediated Ca^{2+} entry is activated by changes of $[Ca^{2+}]_i$ due to the presence of the Ca^{2+} indicator dye. Fura-2 perturbs the *in vivo* Ca^{2+} buffering yielding an increased overall Ca^{2+} buffering capacity. Because TRPV6 channel gating has been shown to strongly depend on the concentrations of intracellular Ca^{2+} chelators, it is likely that changing the Ca^{2+} buffering capacity by any means affects channel opening.

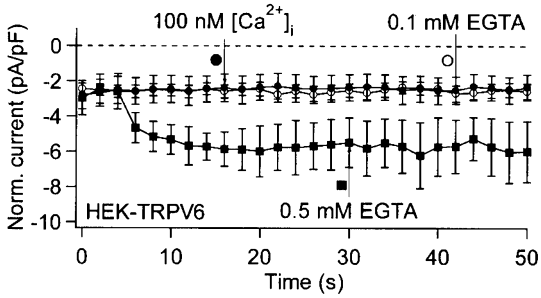

FIG. 2. **Effects of various intracellular buffering conditions on TRPV6-expressing HEK cells.** Time course of inward currents were measured at −80 mV and plotted *versus* the duration of whole cell dialysis. The cesium aspartate-based pipette solution contained either 0.1 mM or 0.5 mM EGTA. The free Ca^{2+} concentration was clamped to 100 nM using EGTA (10 mM) and $CaCl_2$ (3.64 mM). A modified Ringer's solution with 10 mM Ca^{2+} was used extracellularly. The *dashed line* represents zero current. Mean data with double-sided S.E. are shown (n = 9, 7, and 3 for 100 nM free Ca^{2+}, 0.1 mM, and 0.5 mM EGTA, respectively).

Patch-clamp Recordings from TRPV6-expressing Cells Do Not Indicate Spontaneous Channel Activity—Patch-clamp recordings in the whole cell configuration were performed on TRPV6-expressing HEK cells to test this hypothesis. In the presence of a low intracellular EGTA concentration (0.1 mM) a basal current was detectable (Fig. 2). Very similar recordings were obtained from HEK wild-type cells (see below, Fig. 8*C*). However, increasing the chelator concentration slightly (0.5 mM) resulted in the activation of the typical TRPV6 mediated Ca^{2+} influx in transfected cells. The inward current developed rapidly after establishing the whole cell mode and reached small peak current densities after about 20 s (Fig. 2, −6.2 ± 2.0 pA/pF, n = 3). The initial basal current, which was recorded immediately after obtaining the whole cell configuration during the first ramp, had a very small amplitude (Fig. 3*A*) and showed no TRPV6 like current-voltage (I-V) relationship such as the inward rectification and the positive reversal potential (data not shown, n = 7 and 3 for 0.1 and 0.5 mM EGTA, respectively). Considering that in the presence of 0.1 mM EGTA similar currents were obtained both in HEK cells expressing TRPV6 and in HEK cells not expressing TRPV6, it appears unlikely that TRPV6 functions as a spontaneously active channel. Results alike were obtained using RBL cells expressing TRPV6 and RBL cells not expressing TRPV6 (0.1 mM EGTA: n = 7 for RBL-TRPV6 and n = 3 for RBL; 0.5 mM EGTA: n = 8 for RBL-TRPV6 and n = 3 for RBL-wt).

Additional evidence that the basal currents measured after dialyzing the cells with 0.1 mM EGTA are not related to TRPV6 currents comes from experiments where Ca^{2+} was dialyzed into the cell (Fig. 2). According to recent results indicating an inverse correlation of $[Ca^{2+}]_i$ and TRPV6 current activity, one would expect Ca^{2+}-induced current inhibition if TRPV6 forms a constitutive open channel. However, dialyzing Ca^{2+} at a free concentration of 100 nM into TRPV6-expressing HEK cells did not block the inward current (Fig. 2). Similar results were obtained under identical conditions with RBL cells (n = 4 for RBL-TRPV6 and n = 5 for RBL-wt). There was also no difference to the recordings at lower $[Ca^{2+}]_i$ by using 0.1 mM EGTA in the pipette solution from TRPV6-expressing cells HEK (Fig. 2) and RBL cells (n = 7 for RBL-TRPV6 and n = 3 for RBL-wt). In agreement to this, no decrease of the initial inward current was recorded when Ca^{2+} at a free concentration of 1 μM was dialyzed into TRPV6-expressing cells indicating that the basal current recorded in TRPV6-expressing HEK cells is not due to constitutive open TRPV6 channels. Instead, large outward currents with negative reversal potentials were activated in TRPV6-expressing and non-transfected HEK cells, respectively (Fig. 4). In all experiments the inward current was not blocked during the first seconds of each recording, despite the fact that high intracellular concentrations of free Ca^{2+} were used.

Because there was no Ca^{2+}-dependent inhibition of the basal inward current, it seems unlikely that TRPV6 forms open channels when heterologously expressed. Perforated patch-clamp recordings strengthen this conclusion. Cytosolic Ca^{2+} buffers were not affected in these experiments, because the polyen antibiotic nystatin induced holes in the plasma membrane that are too small to allow proteins to permeate. Current densities were not different between TRPV6-expressing HEK cells and HEK cells not expressing TRPV6 (Fig. 3*B*). These results further indicate that TRPV6 channels are closed under resting conditions of physiological Ca^{2+} concentrations. Nevertheless, channel opening might occur by decreasing the Ca^{2+} concentration in the close proximity of the pore, for instance by Ca^{2+} transport out of the cytosol or by increasing the intracellular Ca^{2+} buffer capacity.

TRPV6 Channel Activity Inversely Correlates with the $[Ca^{2+}]_i$—It has been shown before that TRPV6 channel activity depends on the intracellular concentration of EGTA and BAPTA. The influence of the $[Ca^{2+}]_i$ and $[Mg^{2+}]_i$ on TRPV6-mediated Ca^{2+} and monovalent currents has been demonstrated (7). However, chelators such as EGTA, BAPTA, or EDTA do not only bind Ca^{2+} but also other metal ions such as Mg^{2+}, Zn^{2+}, Ni^{2+}, and Co^{2+}. Thus, it is possible that the reduction of other cations rather than a decrease in the $[Ca^{2+}]_i$ led to the activation of TRPV6 channels. Therefore, two sets of experiments were performed with an internal solution containing 10 mM of either EDTA or EGTA together with the appropriate addition of $CaCl_2$ to fix the free Ca^{2+} concentration at 100 nM. Under these conditions, the free concentrations of other metal ions are expected to be different in both intracellular solutions, because the affinities of EDTA and EGTA for most cations is not identical (13). Clamping the $[Ca^{2+}]_i$ at 100 nM in a 10 mM EDTA-containing internal solution resulted in no current activation (Fig. 5). Similarly, dialyzing TRPV6-expressing HEK cells with 100 nM free Ca^{2+} in a 10 mM EGTA-containing solution did not activate Ca^{2+} currents (Fig. 5). Under both conditions the calculated free concentrations of Mg^{2+}, Co^{2+}, Zn^{2+}, Ni^{2+}, or other cations are different. Because no current developed, the gating of TRPV6 channels depends primarily on the $[Ca^{2+}]_i$.

No Spontaneous Activity of Mutant TRPV6 Channels—Ca^{2+} has been shown to inactivate TRPV6 channels in at least two ways: first, there is a prominent and very rapid inactivation like in TRPV5 channels due to local effects of Ca^{2+} on the intracellular pore forming region (14, 15); second, there is an apparent slower inactivation that was found to be dependent on Ca^{2+}-calmodulin binding to the C-terminal domain of human TRPV6 (8). Two mutants of human TRPV6 were used to find out whether constitutive activity is restored in the absence of either mechanism: the truncated variant $TRPV6\Delta_{695–725}$, which lacks the calmodulin binding site and the $TRPV6_{D542A}$ pore mutant, where the aspartate residue at position 542 is replaced by an alanine residue. In TRPV5 from rabbit, the corresponding aspartate residue determines Ca^{2+} permeation and Mg^{2+} block of this channel (14).

Again, no TRPV6 currents were detectable when $TRPV6\Delta_{695–725}$ (Fig. 6, *A* and *B*) or $TRPV6_{D542A}$-expressing cells (Fig. 6, *C* and *D*) were dialyzed using EGTA at 0.1 mM. When the intracellular solution contained 10 mM EGTA, a current readily developed in TRPV6-expressing (Fig. 6*A*) and $TRPV6_{\Delta695–725}$-expressing (Fig. 6*B*) cells, respectively. However, this was not the case in non-transfected HEK cells (Fig.

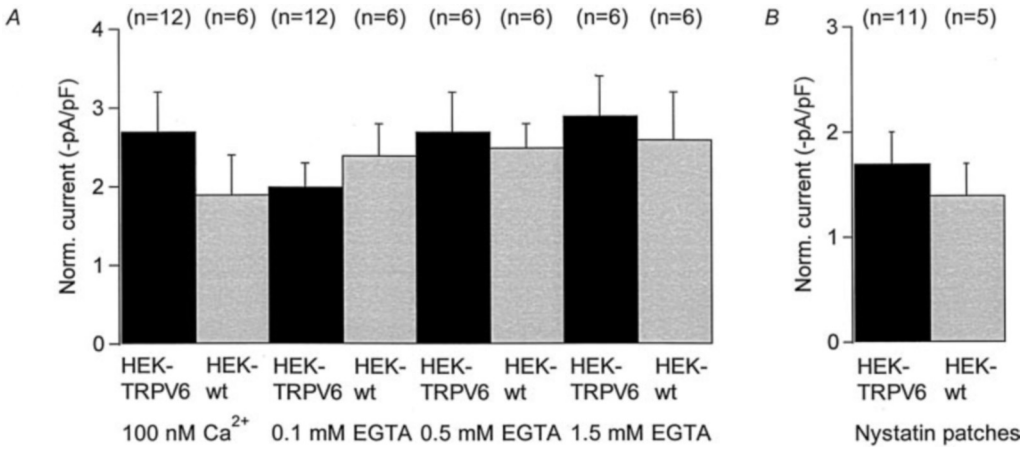

FIG. 3. **Current densities of TRPV6 expressing and non-transfected HEK cells immediately after establishing the whole cell configuration.** *A*, inward currents were measured at −80 mV during the first voltage ramp, which was applied immediately after establishing the whole cell mode. The cesium glutamate-based intracellular solution contained either 0.1, 0.5, or 1.5 mM EGTA. The free Ca^{2+} concentration was clamped at 100 nM by the addition of 10 mM EGTA and 3.64 mM to the standard pipette solution. Initial current densities of −1.7 ± 0.5 pA/picofarad, $n = 5$, were measured if HEDTA was used to buffer the free Ca^{2+} concentration to 100 nM as shown in Fig. 5. *B*, the perforated patch-clamp experiments were performed with the standard pipette solution containing 100 μg ml^{-1} nystatin. Mean data ± S.E. (n) are shown.

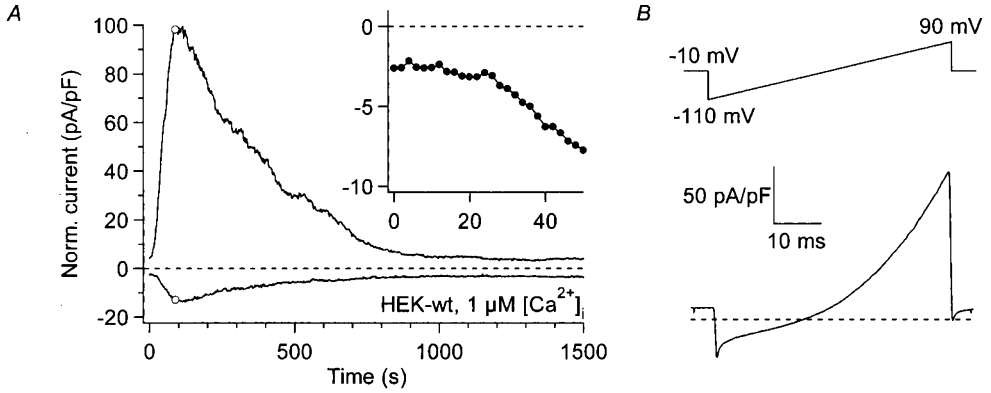

FIG. 4. **Activation and inactivation of an outward current after dialysis of 1 μM Ca^{2+} into a non-transfected HEK cell.** *A*, representative current response of a HEK cell dialyzed with 1 μM Ca^{2+} ($n = 5$). Outward and inward currents were measured at 80 and −80 mV, respectively. The activation of the inward current is shown on an extended time scale in the *inset*. *B*, the I-V curve was recorded at maximal current activation 90 s after establishing the whole cell configuration as indicated in *A*. Similar experiments were performed on TRPV6-expressing HEK cells ($n = 10$).

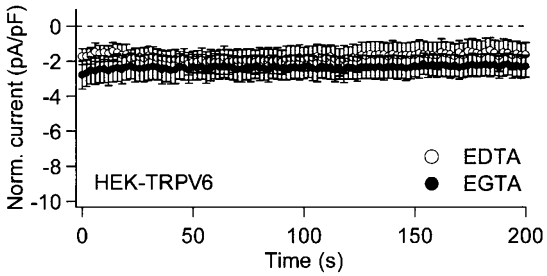

FIG. 5. **Effects of two different intracellular buffering conditions at a fixed $[Ca^{2+}]_i$ on TRPV6-expressing HEK cells.** Experiments were performed as described for Fig. 2 with an intracellular solution containing 10 mM of either EDTA ($n = 5$) or EGTA ($n = 9$).

6*C*) or $TRPV6_{D542A}$-expressing cells (Fig. 6*D*).

The current densities and I-V relations were not different between $TRPV6_{D542A}$ transfected cells and non-transfected cells (Fig. 6, *C* and *D*). Western blots were performed to rule out that the lack of current is due to an impaired or abolished synthesis of the $TRPV6_{D542A}$ protein. As shown in Fig. 7*A* the replacement of aspartate by alanine appears not to interfere with protein synthesis. In addition, the glycosylation pattern is apparently identical in the TRPV6 and the $TRPV6_{D542A}$ proteins arguing against differences in protein processing. Finally, cell surface biotinylation experiments do not show any differences between cell surface expression of TRPV6 and $TRPV6_{D542A}$ (Fig. 7*B*). Several conditions all known to increase TRPV6-mediated currents were tested for their effect on $TRPV6_{D542A}$-expressing HEK cells, including: (i) EGTA or BAPTA at concentrations up to 60 mM were used in the pipette solution; (ii) the cells were depolarized up to holding potentials of 110 mV between ramps; and (iii) conditions were employed to record monovalent currents in the absence of external divalent cations (data not shown). However, the human $TRPV6_{D542A}$ did not express as functional channel.

Activation of TRPV6 Mediated Monovalent Currents in the Absence of Extracellular Divalent Cations at Low Intracellular Ca^{2+} Buffering—TRPV6 channels are highly selective for Ca^{2+} but become permeable to monovalent cations in the absence of extracellular divalent cations (5, 7, 12, 16, 17). In a further series of experiments we investigated whether TRPV6 channels are available for conducting monovalent currents under conditions that do not allow Ca^{2+} to pass the pore in measurable amount. Dialyzing TRPV6-expressing HEK cells with 0.1 mM EGTA induced no activation of inward currents as shown (Figs. 2 and 8). The observed current densities and I-V relationships were indistinguishable to the recordings from non-transfected cells (Fig. 8). However, after removal of divalent cations from the bath solution, a prominent current activated

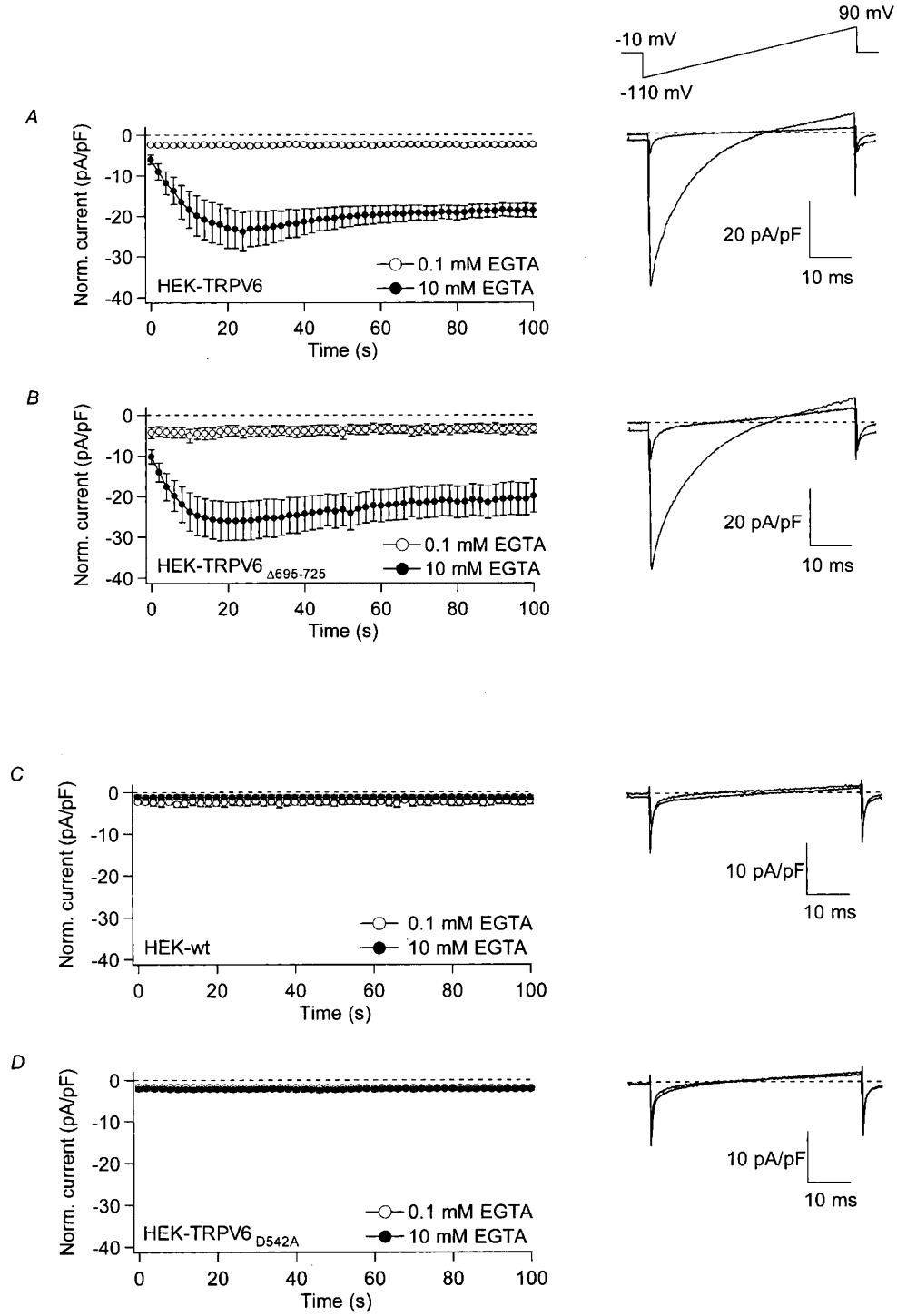

FIG. 6. **Time course of inward currents and I-V curves from HEK cells expressing TRPV6, the truncated TRPV6$_{\Delta 695-725}$, no TRPV6 protein, and the mutant TRPV6$_{D542A}$.** Recordings were carried out with 0.1 or 10 mM intracellular EGTA. The standard bath solution with 10 mM Ca^{2+} was used. Averaged time courses of inward currents are shown with double-sided S.E. on the *left* (*A*, $n = 7$ and 6 HEK-TRPV6 wt for 0.1 and 10 mM EGTA; *B*, $n = 5$ and 4 for HEK-TRPV6$_{\Delta 695-725}$; *C*, $n = 3$ and 6 for HEK-wt; *D*, $n = 18$ and 6 HEK-TRPV6$_{D542A}$). Representative I-V curves were recorded 20 s after establishing the whole cell mode for each EGTA concentration and are shown on the *right-hand side*.

slowly in TRPV6-expressing cells but not in the control cells. The I-V curves were typical for TRPV6-mediated monovalent currents with the strong inward rectification, large current densities, slightly positive reversal potential, and the characteristic negative slope at potentials below −80 mV, which originates from the time- and voltage-dependent removal of the intracellular Mg^{2+} block (7, 17, 18). Re-addition of the Ringer's solution resulted in rapid inactivation of the monovalent current. Apparently the TRPV6 channel is already reluctant or willing for permeation of monovalent cations, which is prevented by the presence of extracellular divalent cations.

DISCUSSION

TRPV6 is a highly Ca^{2+}-selective channel when expressed in HEK cells or in RBL cells, and under most conditions employed so far the TRPV6 proteins have been shown to be spontaneously active. Using whole cell recordings and perforated patch-

clamp experiments we do not detect constitutive open TRPV6 channels at low intracellular Ca^{2+} buffering resembling physiological conditions. However, the removal of divalent cations from the bath solution resulted in the activation of monovalent TRPV6 currents. Previously, it has been shown that Mg^{2+} acts as a bidirectional blocker of mouse TRPV6 currents and that an aspartate residue within the pore of the mouse TRPV6 channel is a crucial determinant of high affinity Ca^{2+} and Mg^{2+} binding responsible for tonic inhibition of the channel (18). Alternatively, the human TRPV6 channel studied here might be blocked by binding of divalent cations not only to the inside of the channel but also to its extracellular domains.

The elevated $[Ca^{2+}]_i$ in TRPV6-expressing HEK cells and the fall of $[Ca^{2+}]_i$ to levels seen in non-transfected cells, if external Ca^{2+} is chelated by EGTA, suggest basal activity as an intrinsic property of the channel (5). However, these recordings were performed using fura-2 AM-loaded cells, and the contribution of the indicator dye on the cytosolic Ca^{2+} buffering capacity has to be considered. By Ca^{2+} binding to fura-2 the $[Ca^{2+}]_i$ can decrease, and thereby, TRPV6-mediated Ca^{2+} entry might be favored. The constitutive activity of TRPV5 (4) observed in the presence of intracellular fura-2 (0.5 mM) and EGTA (0.1 mM) might be explained in a similar way.

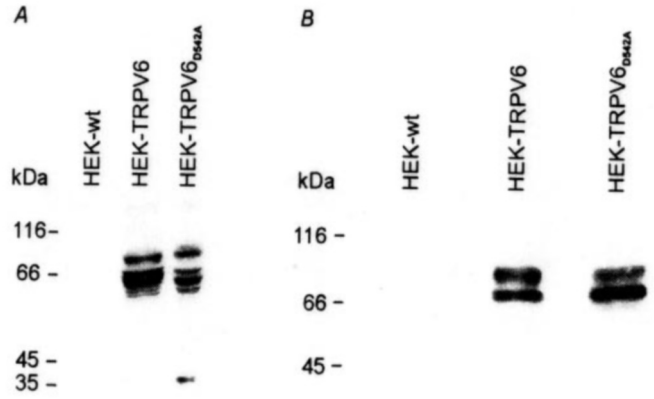

FIG. 7. **Expression of the TRPV6 and TRPV6$_{D542A}$ proteins.** *A*, Western blot of lysate proteins from non-transfected HEK cells and cells expressing either TRPV6 or TRPV6$_{D542A}$. *B*, equal amounts of TRPV6- and TRPV6$_{D542A}$-expressing cells were surface-biotinylated and lysed as described under "Experimental Procedures." Lysates were incubated with avidin-agarose to recover biotinylated proteins, which were separated by electrophoresis, electroblotted, and probed with the anti-TRPV6 antibody.

The presumed pore region of the human TRPV6 protein contains three negatively charged amino acid residues: glutamate (E) at position 535 and aspartates (D) at position 542 and position 550. These residues correspond to residues E534, D541 and D547 in mouse TRPV6 and to residues Glu-535, Asp-542, and Asp-550 in rabbit TRPV5. The aspartate residue responsible for the Mg^{2+} and Ca^{2+} sensitivity is at position 541 in the mouse TRPV6 protein (18) and corresponds to Asp-542 in human TRPV6 and rabbit TRPV5 (14, 19) and to Asp-646 in rat TRPV1 (20). Replacing the aspartate residue at position 542 by an alanine residue in rabbit TRPV5 has recently been shown to abolish Ca^{2+} permeation, Ca^{2+}-dependent current decay, and block by extracellular Mg^{2+}, whereas monovalent cations still permeate the mutant channel (14). Similar results were obtained with the mouse TRPV6$_{D541A}$ mutant (18). Using *Xenopus* oocytes as expression system others demonstrated that the same D542A mutation in rabbit TRPV5 reduces the Ca^{2+}-dependent inhibition of whole cell Li^+ currents by Ca^{2+} (19). After replacing the aspartate residue at position 542 of the human TRPV6 protein by an alanine residue, no functional channels were expressed, although mature glycosylated TRPV6 proteins were readily synthesized, and cell surface expression appears identical for both proteins. Apparently, in human TRPV6 Asp-542 appears to be crucial for channel activity rather than only for its permeation properties as in mouse TRPV6, rabbit TRPV5, or rat TRPV1. The human TRPV6 protein shares 89.7% identical amino acid residues with the mouse protein. Moreover, the putative pore region of the mouse clone contained an additional aspartate residue at position 547, which is not conserved in human. Accordingly these differences of amino acid sequences might contribute to the functional roles of Asp-542 and Asp-541 in the human and mouse proteins, respectively.

In summary, human TRPV6 functions as a Ca^{2+}-selective channel that is closed at physiological $[Ca^{2+}]_i$ when studied as a recombinant channel in HEK cells. Activation of the channel requires one of the following conditions: (i) the removal of the

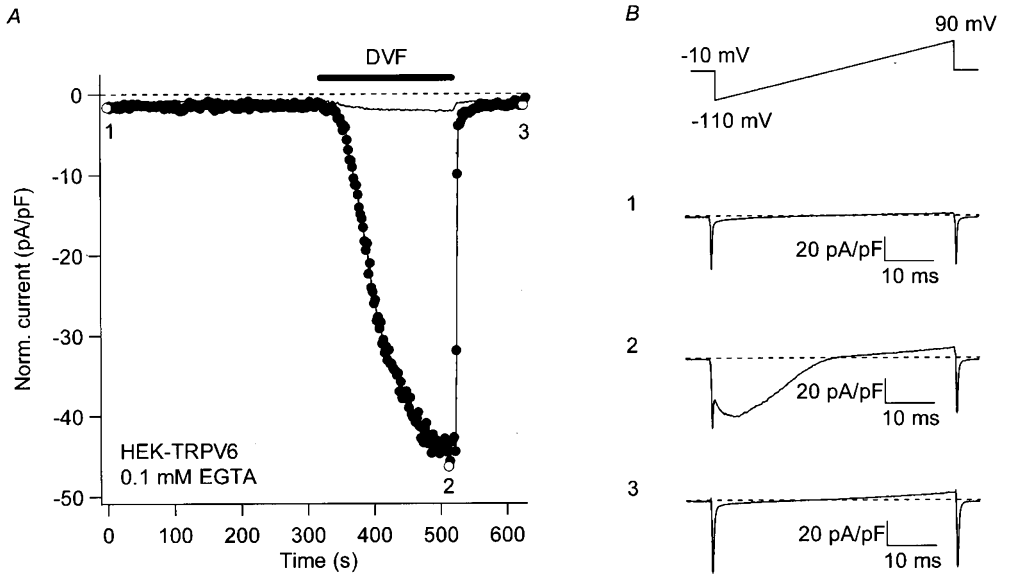

FIG. 8. **Activation of TRPV6-mediated monovalent currents in the absence of extracellular divalent cations at low intracellular Ca^{2+} buffering.** *A*, time course of currents from a representative TRPV6-expressing HEK cell dialyzed with an intracellular solution containing 0.1 mM EGTA and 6 mM Mg-ATP ($n = 4$). The divalent-free solution was applied, as indicated with the *bar*. The typical response of a non-transfected HEK cell is shown in *gray* ($n = 4$). *B*, I-V curves were obtained during the experiment shown in *A* as indicated.

intracellular Ca^{2+} and/or Mg^{2+} block, (ii) plasma membrane depolarization, or (iii) the absence of extracellular divalent cations. Interaction of TRPV6 and TRPV5 (21) is another potential mechanism for channel regulation that may affect the gating of both channels. The first two activation mechanisms seem to be most conceivable under physiological conditions. Ca^{2+} extrusion proteins such as Ca^{2+} ATPases in the plasma membrane and endoplasmic reticulum or cytosolic Ca^{2+} buffers like calbindin can increase the driving force. Thereby TRPV6-dependent Ca^{2+} influx is attenuated, because the negative feedback of the incoming Ca^{2+} on channel activity is reduced. For TRPV5 a colocalization with calbindin D_{9k} has been shown (6) and a regulation of TRPV5 and TRPV6 protein expression by 1,25-dihydroxyvitamin D_3 was reported (1, 6, 12). However, functional data on TRPV5 and TRPV6 channels from primary cells are still missing to support the idea of TRPV5 and TRPV6 being Ca^{2+} entry channels responsible for epithelial Ca^{2+} uptake during intestinal Ca^{2+} absorption and renal Ca^{2+} reabsorption. Whether this voltage dependence of TRPV6 takes place under *in vivo* Ca^{2+} buffering and at physiological changes in the membrane potential needs further evaluation.

Acknowledgments—We thank Heidi Löhr for excellent technical assistance. This work was supported, in part, by the Wilhelm Sander-Stiftung and the Fonds der Chemischen Industrie.

REFERENCES

1. Peng, J. B., Brown, E. M., and Hediger, M. A. (2003) *J. Physiol.* **551,** 729–740
2. Hoenderop, J. G., van der Kemp, A. W., Hartog, A., van de Graaf, S. F., van Os, C. H., Willems, P. H., and Bindels, R. J. (1999) *J. Biol. Chem.* **274,** 8375–8378
3. Peng, J. B., Chen, X. Z., Berger, U. V., Vassilev, P. M., Tsukaguchi, H., Brown, E. M., and Hediger, M. A. (1999) *J. Biol. Chem.* **274,** 22739–22746
4. Vennekens, R., Hoenderop, J. G., Prenen, J., Stuiver, M., Willems, P. H., Droogmans, G., Nilius, B., and Bindels, R. J. (2000) *J. Biol. Chem.* **275,** 3963–3969
5. Wissenbach, U., Niemeyer, B. A., Fixemer, T., Schneidewind, A., Trost, C., Cavalie, A., Reus, K., Meese, E., Bonkhoff, H., and Flockerzi, V. (2001) *J. Biol. Chem.* **276,** 19461–19468
6. Hoenderop, J. G., Nilius, B., and Bindels, R. J. (2002) *Biochim. Biophys. Acta* **1600,** 6–11
7. Bödding, M., Wissenbach, U., and Flockerzi, V. (2002) *J. Biol. Chem.* **277,** 36656–36664
8. Niemeyer, B. A., Bergs, C., Wissenbach, U., Flockerzi, V., and Trost, C. (2001) *Proc. Natl. Acad. Sci. U. S. A.* **98,** 3600–3605
9. Hirnet, D., Olausson, J., Fecher-Trost, C., Bödding, M., Nastainczyk, W., Wissenbach, U., Flockerzi, V., and Freichel, M. (2003) *Cell Calcium* **33,** 509–518
10. Hamill, O. P., Marty, A., Neher, E., Sakmann, B., and Sigworth, F. J. (1981) *Pflügers Arch.* **391,** 85–100
11. Horn, R., and Marty, A. (1988) *J. Gen. Physiol.* **92,** 145–159
12. Bödding, M., Fecher-Trost, C., and Flockerzi, V. (2003) *J. Biol. Chem.* **278,** 50872–50879
13. Martell, A. E., and Smith, R. M. (1974) *Critical Stability Constants*, Vol. 1, Plenum Press, New York
14. Nilius, B., Vennekens, R., Prenen, J., Hoenderop, J. G., Droogmans, G., and Bindels, R. J. (2001) *J. Biol. Chem.* **276,** 1020–1025
15. Nilius, B., Vennekens, R., Prenen, J., Hoenderop, J. G., Bindels, R. J., and Droogmans, G. (2000) *J. Physiol.* **527,** 239–248
16. Yue, L., Peng, J. B., Hediger, M. A., and Clapham, D. E. (2001) *Nature* **410,** 705–709
17. Voets, T., Prenen, J., Fleig, A., Vennekens, R., Watanabe, H., Hoenderop, J. G., Bindels, R. J., Droogmans, G., Penner, R., and Nilius, B. (2001) *J. Biol. Chem.* **276,** 47767–47770
18. Voets, T., Janssens, A., Prenen, J., Droogmans, G., and Nilius, B. (2003) *J. Gen. Physiol.* **121,** 245–260
19. Jean, K., Bernatchez, G., Klein, H., Garneau, L., Sauve, R., and Parent, L. (2002) *Am. J. Physiol.* **282,** C665–C672
20. Garcia-Martinez, C., Morenilla-Palao, C., Planells-Cases, R., Merino, J. M., and Ferrer-Montiel, A. (2000) *J. Biol. Chem.* **275,** 32552–32558
21. Hoenderop, J. G. J., Voets, T., Hoefs, S., Weidema, F., Prenen, J., Nilius, B., and Bindels, R. J. M. (2003) *EMBO J.* **22,** 776–785